Heliyon 9 (2023) e13834

Contents lists available at ScienceDirect

Heliyon

journal homepage: www.cell.com/heliyon

Research article

Physicochemical properties of intact fungal cell wall determine vesicles release and nanoparticles internalization

Hoda Ebrahimi [a], Farideh Siavoshi [a,*], Mir Hadi Jazayeri [b,c], Abdolfattah Sarrafnejad [d], Parastoo Saniee [e], Maryam Mobini [d]

[a] Department of Microbiology, School of Biology, University College of Sciences, University of Tehran, Tehran, Iran
[b] Department of Immunology, Faculty of Medical Sciences, Iran University of Medical Sciences, Tehran, Iran
[c] Immunology Research Center, Iran University of Medical Sciences, Tehran, Iran
[d] Department of Immunology, School of Public Health, Tehran University of Medical Sciences, Tehran, Iran
[e] Department of Microbiology and Microbial Biotechnology, Faculty of Life Science and Biotechnology, Shahid Beheshti University, Tehran, Iran

ARTICLE INFO

Keywords:
Yeast
Extracellular vesicles
Cell wall pores
Flexibility
Nanoparticles release
Internalization

ABSTRACT

Our previous microscopic observations on the wet mount of cultured Candida yeast showed release of large extracellular vesicles (EVs) that contained intracellular bacteria (~500–5000 nm). We used *Candida tropicalis,* to examine the internalization of nanoparticles (NPs) with different properties to find out whether the size and flexibility of both EVs and cell wall pores play role in transport of large particles across the cell wall.

Candida tropicalis was cultured in *N*-acetylglucoseamine-yeast extract broth (NYB) and examined for release of EVs every 12 h by the light microscope. The yeast was also cultured in NYB supplemented with of 0.1%, 0.01% of Fluorescein isothiocyanate (FITC)-labelled NPs; gold (0.508 mM/L and 0.051 mM/L) (45, 70 and 100 nm), albumin (0.0015 mM/L and 0.015 mM/L) (100 nm) and Fluospheres (0.2 and 0.02%) (1000 and 2000 nm). Internalization of NPs was recorded with fluorescence microscope after 30 s to 120 min. Release of EVs mostly occurred at 36 h and concentration of 0.1% was the best for internalization of NPs that occurred at 30 s after treatment. Positively charged 45 nm NPs internalized into >90% of yeasts but 100 nm gold NPs destroyed them. However, 70 nm gold and 100 nm negatively-charged albumin were internalized into <10% of yeasts without destroying them. Inert Fluospheres either remained intact on the surface of yeasts or became degraded and internalized into ~100% of yeasts. Release of large EVs from the yeast but internalization of 45 nm NPs indicated that flexibility of EVs and cell wall pores as well as physicochemical properties of NPs determine transport across the cell wall.

1. Introduction

Fungal cell wall was first described as a rigid basket-like scaffold around the cell that conferred resistance to hydrostatic pressure exerted by the cell cytoplasm and membrane. However, results of further investigations on fungal cell wall architecture and composition revealed a complex structure with unique physicochemical properties that could have evolved for much more sophisticated functions [1]. Recent studies indicate that fungal cell wall is one of the most complex and highly regulated structures in microbial

* Corresponding author.
E-mail address: siavoshi@khayam.ut.ac.ir (F. Siavoshi).

https://doi.org/10.1016/j.heliyon.2023.e13834
Received 20 August 2022; Received in revised form 12 February 2023; Accepted 14 February 2023
Available online 17 February 2023
2405-8440/© 2023 The Authors. Published by Elsevier Ltd. This is an open access article under the CC BY-NC-ND license (http://creativecommons.org/licenses/by-nc-nd/4.0/).

world that plays an absolutely fundamental role in fungal nutrient acquisition and adaptation to a versatile range of habitats. These could not have been fulfilled without cell wall properties such as negative charge for absorption of cations [2], hydrophobicity for adhesion to the surfaces [3], flexible viscoelasticity for rapid remodelling into hyphae or bud [4] and adjusting porosity to limit the entry of large particles [5] while facilitating vesicular transport [6].

Fungal cell wall is a two-layered structure, the inner cell wall composed of β-glucans and chitin, confers strength and physical shape to the wall. The outer cell wall, in *Candida albicans*, is made of a fibrillar layer of highly glycosylated mannoproteins that determine the physical properties of the cell wall such as negative charge and viscoelasticity [7] as well as hydrophobicity, porosity, adhesiveness and immunologic characteristic [8]. Mannoproteins in Candida also protect fungal cell against host's enzymes and antimicrobials, macrophage phagocytosis and immune response to underlying β-1, 3-glucan layer [9]. In addition to major components of the fungal cell wall, hydrolytic enzymes; phospholipases, proteinases, lipases, esterases and hemolysin are secreted for degradation of nutrients [10].

Despite acting as a rigid scaffold for protecting the protoplasm, fungal cell wall has been specialized for facilitating transport into and out of the fungal cell. In fungi, while absorbed small molecules can freely pass the cell wall and reach the cell membrane, large nutrients are digested into smaller molecules by secretory enzymes and then absorbed into the cell. On the other hand, export of fungal products across the cell wall is facilitated by extracellular vesicles (EVs) that traverse the cell wall pores [6]. EVs are membrane-bound structures that are released to the external environment by all the living cells [11] and mediate intercellular communications [12]. They exhibit different morphologies [13] and carry different cargos [14]. Reports indicate that EVs play important roles in the fungal biology and pathogenesis [15].

It has been suggested that flexibility of cell wall pore and EVs is part of the control system for in and out cellular traffic in fungi. On the one hand, the size of cell wall pores in *Saccharomyces cerevisiae* has been measured between 200 and 400 nm [16]. On the other hand, the size of EVs that traverse the cell wall has been estimated as 60–300 nm in *Cryptococcus neoformans* [17], 50–500 nm in *S. cerevisiae* [18] and 50–800 nm in *C. albicans* [19]. By observing that the size of fungal exported vesicles often exceeded the exclusion size estimated for cell wall permeability, it was suggested that EVs with lipid bilayer structure may compress to traverse the cell wall pores smaller than their diameter [6]. Furthermore, cell wall pores may enlarge under stressful conditions due to their flexible viscoelastic properties. These data indicate that size, flexibility and probably other properties of the cell wall pores and EVs may be involved in traffic across the fungal cell wall [4].

Results of our previous studies showed the endosymbiotic relationship between *H. pylori* with Candida yeast. Intracellular occurrence of *H. pylori* inside the vacuole of yeast was demonstrated by microscopy and molecular methods [20,21]. It was proposed that yeast could protect the endosymbiotic bacteria from environmental stresses and provide them with nutrients. The outcome of this mutual relationship would be survival of both partners under stressful conditions and residing in a wide range of habitats. It was suggested that Candida yeast that occurs in nature, food and mucosal surfaces of human body may serve as a potent reservoir of *H. pylori* that facilitates bacterial spread in the environment and within human hosts [22]. However, the important question that remained was how are bacteria released from the yeast? In the other words, is there an effective mechanism for release of the intracellular *H. pylori*?

In our recent study, examination of a gastric *Candida albicans* in liquid culture by light, fluorescence and transmission electron microscopy revealed that yeast cells released EVs with various size and morphology that contained bacteria. Using immunogold labelling method, we detected *H. pylori*-specific proteins in the vesicles' membrane. Furthermore, release of free *H. pylori* from yeast was documented by immunomagnetic separation and detection of *H. pylori*-specific 16S rDNA in bead-bound bacteria and sequencing [19]. Our results were in accordance with other reports that showed release of vesicles from protozoa that contained intracellular bacteria such as *Escherichia coli* O157 [23], *Listeria monocytogenes* [24] and *Salmonella enterica* [25]. Furthermore, release of free bacteria such as *Legionella pneumophila* [26] and mycobacteria [27] from intact amoeba host has been reported. Release of intracellular bacteria as free or encased in EVs have been regarded as peaceful strategies, compared with lytic escape of intracellular bacteria that destroys the host cell [28,29]. Interestingly, it has been demonstrated that large structures such as bacterial cells may also pass through the cell wall pores, internalize into fungal cell and establish endosymbiotic relationship [30].

In the present study, examination of wet mount preparations from the liquid culture of *Candida tropicalis* by the light microscope showed release of large EVs with different morphology. We observed EVs that carried visible dense cargos that resembled intracellular bacteria we observed previously. Considering the published size of fungal cell wall pores (200–400 nm), EVs (50–800 nm) and bacterial cell (rods: 2000–5000 nm × 500–1000 nm and cocci: 500–1000 nm), these observations raised the question about the flexibility of cell wall pores that allowed the exit of large EVs with intracellular bacteria. Here, we estimated the approximate size of the cell wall pores by examining the internalization of Fluorescein isothiocyanate (FITC)-labelled nanoparticles (NPs) with different diameters into the vacuole of intact yeast cell. FITC-labelled gold NPs with the size of 45, 70 and 100 nm and FITC-labelled albumin NPs with the size of 100 nm were prepared. Furthermore, two commercially- manufactured Fluospheres with the size of 1000 and 2000 nm were purchased. Fluorescence microscope was used for localizing the internalized NPs inside yeast's vacuole, using different concentrations of NPs and exposure time. We looked for the internalized NPs in yeast's vacuole, because results of our previous study showed that FITC-labelled antibodies entered the yeast by endocytosis and localized inside the vacuole [31].

2. Materials and methods

2.1. Yeast strains for release of extracellular vesicles and internalization of nanoparticles

Two yeast isolates (A and B) from cultures of gastric biopsies of two dyspeptic patients on brucella blood agar were used in this

study. Isolated yeasts were purified by subculturing a single colony of yeasts on homemade yeast extract- glucose (YG) agar containing yeast extract (0.5%) (Pronadisa, Spain), glucose (2%) and agar (1.5%) (pH 7). Yeast isolates were identified according to their colony morphology on YG agar, colony colour on CHROMagar (CHROMagar, France) and formation of blastoconidia in *N*-acetylglucoseamine-yeast extract broth (NYB) composed of 20 g/L *N*-acetylglucoseamine (Sigma, USA) and 5 g/L yeast extract (pH 7). Cultures were incubated at 30 °C for 24–48 h. Yeast A and B were identified as members of the Candida genus according to their cream-coloured, dull and smooth colonies on YG agar as well as production of blastoconidia in NYB. Yeast A was identified as *C. tropicalis* due to production of turquoise blue colonies on CHROMagar and yeast B as *C. albicans* due to production of green colonies on CHROMagar. Amplification of D1/D2 region of 26S rDNA from A and B yeasts was carried out according to Carvalho et al. using primers NL1 (5′-GCATATCAATAAGCGGAGGAAAAG-3′) and NL4 (5′-GGTCCGTGTTTCAAGACGC-3′) [32]. Amplified 600-bp products were sequenced and matched with the sequences in the GenBank database. The results confirmed the identity of yeast A as *Candida tropicalis* and yeast B as *Candida albicans*. *C. tropicalis* was used in all the steps of NPs internalization studies and *C. albicans* was used for comparison. For observing release of EVs, *C. tropicalis* was cultured in NYB and incubated as mentioned above. Wet mounts were prepared from *C. tropicalis* culture every 12 h and examined by the light microscope for observing release of EVs.

2.2. Preparation of FITC-labelled nanoparticles

NPs used in this study included home-made gold particles (45, 70 and 100 nm) with irregular shape and positive charge, albumin (Bio Basic, D0024) (100 nm) particles with spherical shape and negative charge and commercially purchased inert spherical Fluospheres (Thermofisher Scientific, USA). Gold NPs with different size were synthesized, using citrate reduction of chloroauric acid ($HAuCl_4$), according to Frens [33]. Briefly, different volumes (45, 70 and 100 mL) of 1% $HAuCl_4$ (Sigma) were heated and stirred until reaching boiling point. Volumes of 0.9 mL, 0.6 mL and 0.4 mL of 1% tri-sodium citrate (Merck, Germany) solution were added to 45, 70 and 100 mL of boiling 1% chloroauric acid, respectively. Appearance of grey colour within few minutes that changed to pink indicated the formation of the stable gold NPs. Mixtures were allowed to boil for another 5 min, cooled quickly to room temperature and stored at 4 °C until used. Estimation of hydrodynamic diameter of synthesized gold NPs by dynamic light scattering showed that the average size of over 90% of gold NPs was about 45, 70 and 100 nm [33]. Nanoparticle size was confirmed by UV–Vis Spectra according to Haiss and et al. [34]. Scale bar result for nanoparticle's size of 45 nm is presented as an example (Fig. 1). FITC labelling was done by dropwise adding FITC (0.4 mg in 8 mL ethanol) to the original solution of each gold NP until appearance of orange colour. Excess ethanol was evaporated while shaking (200 rpm) at room temperature in the dark for 1 h. Labelled particles were harvested by centrifugation (6000 rpm) for 5 min, washed twice with 1X phosphate-buffered saline (PBS) and resuspended in 500 μL of PBS as the original solutions of NPs [35,36]. The original solutions of all gold NPs were 1/10 twice diluted to reach the concentrations of 0.1% (0.508 mM/L) and 0.01% (0.051 mM/L) by every time adding 15 μL of the NPs solutions to tubes containing 135 μL of fresh NYB and mixing thoroughly by pipetting.

Albumin NPs with the size of 100 nm were made according to Zhang by dissolving 10 mg of serum albumin powder in 1 mL of sterilized distilled water. FITC labelling was done by dropwise adding FITC (0.4 mg in 8 mL ethanol) to albumin solution until grey precipitate of the FITC-labelled albumin formed. To fix the label, FITC-albumin was treated with 25 μL of 0.25% glutaraldehyde for 30 min. Excess ethanol was evaporated while shaking (200 rpm) at room temperature in dark for 1 h [37]. Finally, albumin NPs were harvested by centrifugation (15,000 rpm) for 5 min, washed twice with 1X PBS and resuspended in 500 μL of PBS as the original solution of NPs. The original solutions of albumin NPs were 1/10 twice diluted to reach the concentrations of 0.1% (0.0015 mM/L) and 0.01% (0.015 mM/L) by every time adding 15 μL of the NPs solutions to tubes containing 135 μL of fresh NYB and mixing thoroughly by pipetting.

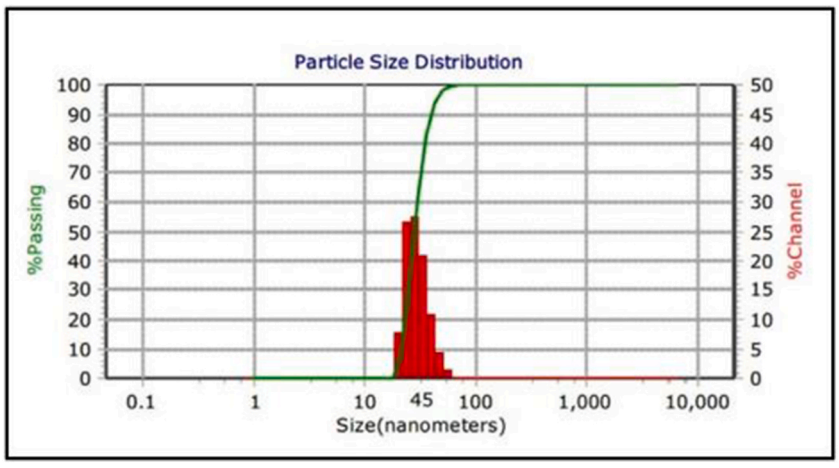

Fig. 1. UV–vis spectrum of synthesized 45 nm gold nanoparticles. (For interpretation of the references to colour in this figure legend, the reader is referred to the Web version of this article.)

NPs with the size of 1000 and 2000 nm and concentration of 2% were purchased in their labelled forms with commercial name of Fluospheres. The manufacturer described Fluospheres as polysterene particles covered with carboxylic acid. Fluospheres were washed with Tris-NaCl (15 mM NaCl in 50 mM Tris- HCl, pH 7.6) and resuspended in 500 μL Tris-NaCl before use [38]. Examination of Fluospheres, with light and fluorescence microscopes showed that all Fluospheres were homogenous in size and there were absolutely no smaller particles as shown in Fig. 4. The original solutions of Fluospheres were 1/10 twice diluted to reach the concentrations of 0.2 and 0.02% by every time adding 15 μL of the NPs solutions to tubes containing 135 μL of fresh NYB and mixing thoroughly by pipetting.

2.3. Internalization of NPs into Candida tropicalis- impact of NPs concentration and exposure time

Tubes containing different concentrations of NPs were inoculated with 10 μL of fresh *Candida tropicalis* culture in NYB (6×10^6 cells/CFU). Tubes were incubated at 30 °C while shaking (250 rpm) and examined by fluorescence microscope for internalization of NPs after different times (30 s–120 min). Five μL of 0.01% evans blue was added to each tube for contrast and wet mounts were prepared in dark. Untreated *C. tropicalis* was similarly stained with evans blue and used as a control. *C. albicans* was similarly treated with 70 and 100 nm gold nanoparticles as well as 1000 and 2000 nm Fluospheres. Treated yeasts were also Gram-stained and examined by the light microscope for their structural integrity. For viability test, a drop of NPs - treated *C. tropicalis* cultures was surface inoculated on brain heart infusion (BHI) agar (Pronadisa, Spain) and examined for growth up to one week of incubation at 30 °C.

2.4. Utilization of fluospheres as carbon source

By observing that both *Candida tropicalis* and *Candida albicans* internalized Fluospheres by first degrading them into smaller particles, Fluospheres were added to a solid medium as the sole supplement and carbon source. A 30-μL volume of each Fluosphere's original solution was added to 1.5 g agar (Pronadisa, Spain) solution in 100 mL of distilled water which was sterilized and cooled to 45 °C. The solidified media of two Fluospheres were surface inoculated with *C. tropicalis* (6×10^6 cells/CFU), incubated at 30 °C and examined for growth up to 48 h. Culture of *C. tropicalis* on pure agar, without a carbon source, was used as a control.

3. Results and discussion

Results of our recent study demonstrated the release of free or vesicle-encased *H. pylori* from Candida yeast that was not culturable [19]. Results of our previous studies showed release of different intracellular bacteria from gastric yeasts under stressful conditions: *Staphylococcus xylosus*, *S. haemolyticus*, *Arthrobacter parietis* and *Cellulomonas hominis* under starvation [19] *Nocardia nova* [39] and *Leptolyngbya boryana* [40] due to aging and *S. hominis* and *S. haemolyticus* due to exposure to antifungal amphotericin B [41]. The released bacteria were culturable under laboratory conditions and their intracellular occurrence was documented by light and fluorescence microscopy and detection of prokaryotic 16S rDNA and sequencing. These results showed release of large bacterial cells, free or vesicle-encased, through the fungal cell wall. Aim of this study was to estimate whether the size of cell wall pores was large enough to allow the export of free or vesicle-encased bacteria.

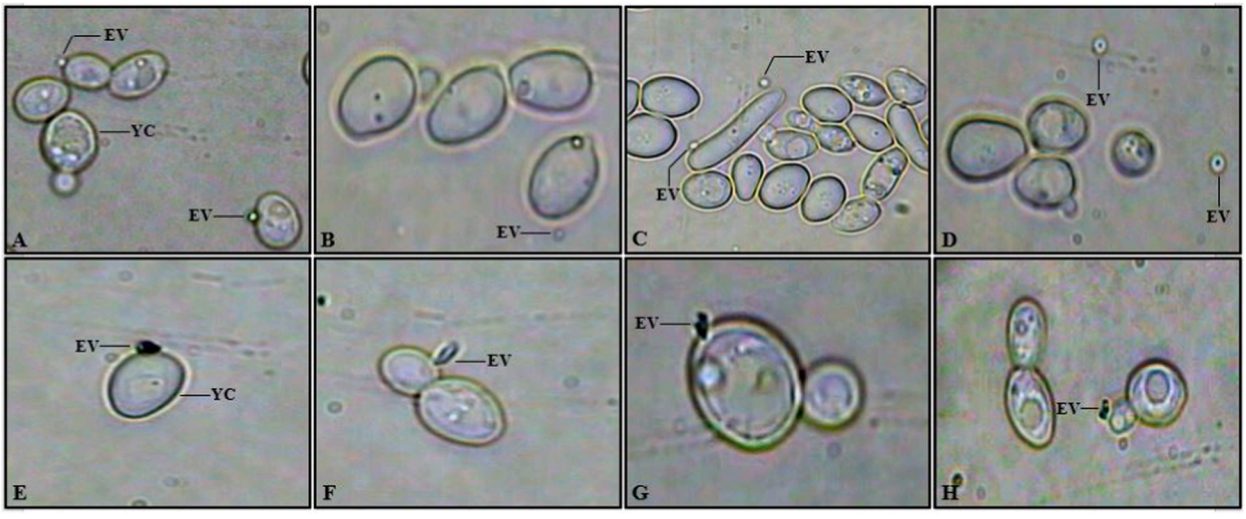

Fig. 2. Release of extracellular vesicle (EV) from *Candida tropicalis*. Light microscopy observations showed release of round (A–D) or polymorphous (E–H) EVs from yeast cell (YC). Original magnification: × 1250.

3.1. Release of extracellular vesicles from Candida tropicalis

In this study, examination of a wet mount preparation from liquid culture of *Candida tropicalis* by the light microscope showed release of EVs from yeast cells at about 36 h. Released EVs had large size and different morphologies and some carried intracellular bacteria (Fig. 2). Release of large EVs through the fungal cell wall indicated that membranous EVs were large and flexible enough to encase the bacterial cell and carry it through the cell wall. Furthermore, the flexible cell wall pores that could enlarge under the stressful conditions, readjusted to allow the release of vesicles. Results of the present study revealed that fungal EVs and cell wall pores readjust their size to allow the transport of large particles such as bacteria. Release of EVs in *Cryptococcus neoformans*, *Paracoccidioides brasiliensis*, *Saccharomyces cerevisiae*, and *C. albicans* [42]. The lipid bilayer of EVs is a stable structure that protects their contents from degradation and mediates their delivery to a new target cell [43].

3.2. Internalization of FITC- NPs and fluospheres into Candida tropicalis

3.2.1. Concentration of nanoparticles and exposure time

Fluorescence microscopy observations on *Candida tropicalis* showed that concentration of 0.1% was the best for all NPs to internalize into the vacuole of yeast cells (Fig. 3). Furthermore, internalization of all NPs occurred at 30 s after treatment of yeast and except for Fluospheres, did not change by longer exposure time (Fig. 4A–C).

3.2.2. Internalization of gold NPs

Fluorescence microscopy observations of *Candida tropicalis* that were treated with FITC-labelled gold NPs showed that irregularly-shaped and positively-charged gold NPs with 45 and 70 nm size internalized into yeast cells. Photograph of untreated yeast cells that stained red with evans blue showed the contrast due to the internalization of NPs (Fig. 3E). Internalization of 45 nm gold NPs was observed in a considerable number of yeast cells (>%90) (Fig. 3A and A′). However, 70 nm gold NPs were observed in a fewer number of yeast cells (<%10) (Fig. 3B and B′), indicating restricted internalization due to their large size as well as positive charge that led to aggregation with cell wall components and reduced permeability. TEM observations on *S. cerevisiae* cells treated with 15–20 nm gold NPs showed decrease in gold accumulation as the concentration of gold increased, suggesting restriction of cell wall permeability to

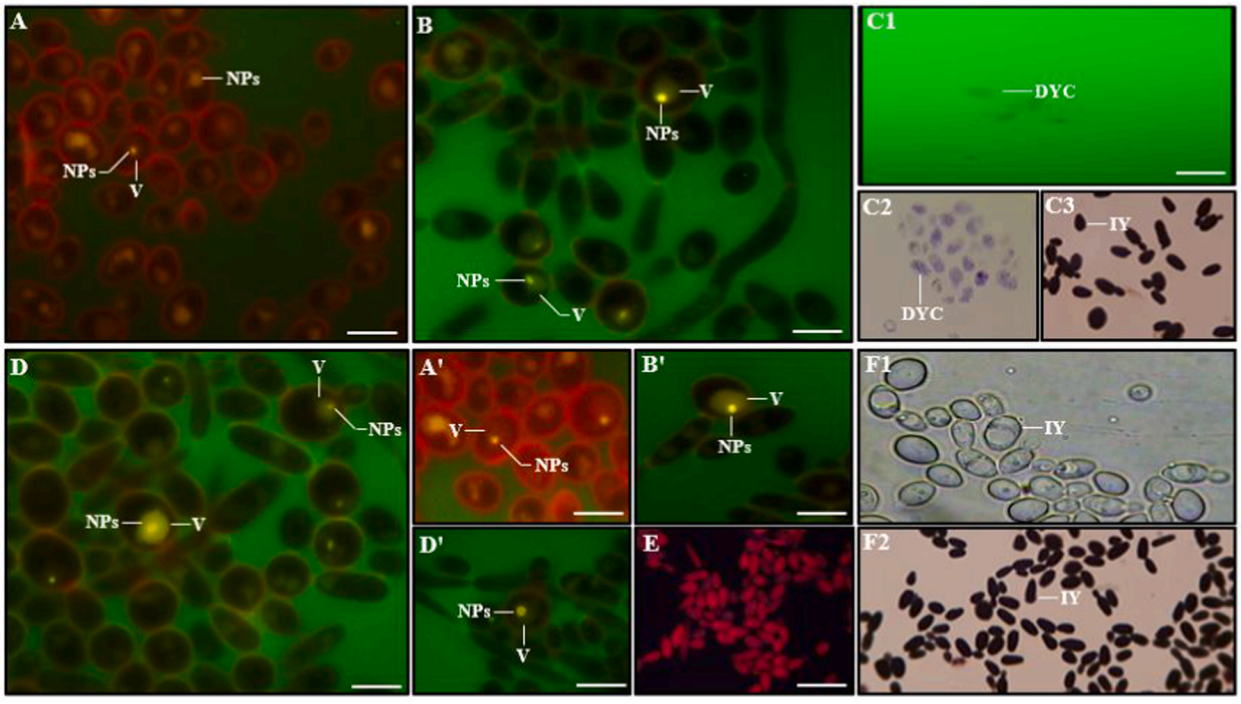

Fig. 3. Fluorescence microscopy of *Candida tropicalis* exposed to FITC-labelled 45, 70 and 100 nm gold and 100 nm albumin nanoparticles (NPs). A and A′) Internalization of 45 nm gold NPs into the vacuole (V) of yeast cells. B and B′) Internalization of 70 nm gold NPs into the vacuole (V) of yeast cells. Fluorescence (C1) and light (C2) microscopy of yeasts exposed to 100 nm gold NPs showed ghosts of destroyed yeast cells (DYCs), compared with a Gram- stained preparation of intact yeasts (IY) as a control (C3). D and D′) Internalization of 100 nm albumin NPs into the vacuole (V) of yeast cells. E) Untreated yeast cells stained red with evans bule. Wet mount (F1) and Gram- stained (F2) preparations of yeasts treated with 45 and 70 nm gold NPs and 100 nm albumin NPs showed intact yeasts (IY) after exposure to NPs. Original magnification of A, A′, B, B′ C1, D, D′ and E: × 1000. Original magnification of C2, C3, F1 and F2: × 1250. Scale Bar: 5 μm. (For interpretation of the references to colour in this figure legend, the reader is referred to the Web version of this article.)

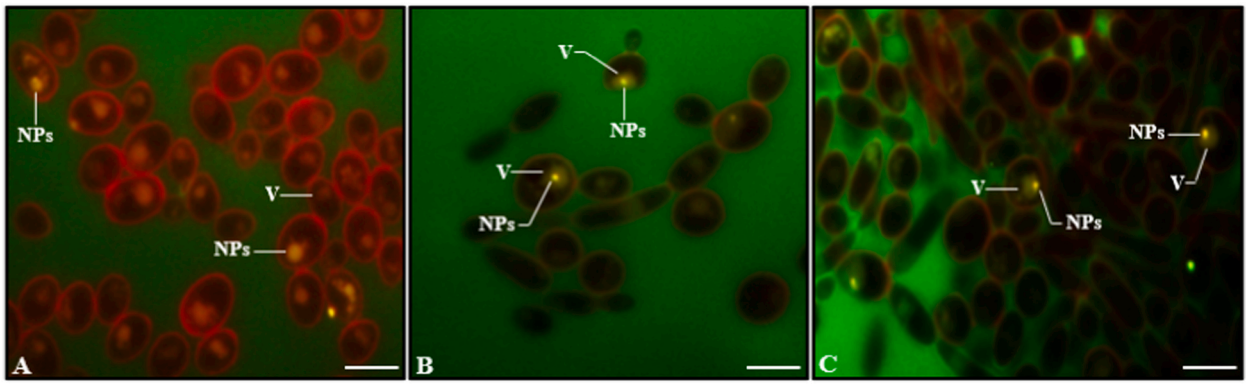

Fig. 4. Internalization of FITC-labelled nanoparticles (NPs) into *Candida tropicalis* after longer exposure. Internalization of 45 (A) and 70 nm gold NPs (B) and 100 nm albumin NPs (C) into the yeast vacuole (V) did not change after longer exposure time. Original magnification × 1000. Scale Bar: 5 μm. (For interpretation of the references to colour in this figure legend, the reader is referred to the Web version of this article.)

high amounts of foreign particles. It was found that internalization of gold NPs did not affect the viability of yeast as demonstrated by their growth on solid medium [2]. It has been shown that bivalent cations form bridges between multiple negative charged phosphate groups in mannoproteins in yeast cell wall, reducing the cell wall permeability [44]. Furthermore, treatment of *C. neoformance* with bivalent cations, such as Ca^{2+} led to aggregation of surface polysaccharide molecules due to formation of inter- or intra-molecular bridges [45], reducing fungal permeability to immunoglobulin penetration [46]. Light microscopy observations on Gram-stained preparations of yeasts exposed to 45 and 70 nm gold NPs showed intact cell structure (Fig. 3F1 and F2). These yeasts retained their viability and grew on BHI agar. Fluorescence microscopy of yeasts exposed to 100 nm gold NPs showed only the ghosts of destroyed yeast cells against fluorescent green background due to FITC- gold NPs (Fig. 3C1). Examination of Gram-stained yeasts by the light microscope showed destruction of yeast cells and their culture on BHI agar was negative (Fig. 3C2 and C3). Gold 100 nm NPs were not toxic by themselves because they were prepared from the same stock as 45 and 70 nm gold NPs. Internalization of 70 nm gold NPs was similarly observed in only few *C. albicans* yeasts (<%10) (Fig. 5A and A′). Treatment of *C. albicans* with 100 nm gold NPs led to destruction of yeast cells (data not shown).

3.2.3. Internalization of albumin NPs

Fluorescence microscopy observation on *Candida tropicalis* and *Candida albicans* that were treated with negatively charged and spherical 100 nm albumin NPs, showed only a few yeasts with NPs adhered to the surface or internalized into the vacuole of yeast (<% 10) (Fig. 3D and D′). This could be due to their negative charge and large size that reduced particle internalization. Gram-stained preparation of these yeasts showed their intact cell structure (Fig. 3F1 and F2) and their culture on BHI agar was positive (data not shown).

3.2.4. Internalization of fluospheres

Fluorescence microscopy observations on Fluosphere-treated *Candida tropicalis* and *Candida albicans* showed that inert and spherical carboxylated polysterene Fluospheres with 1000 and 2000 nm diameters either remained intact and adhered to the surface of

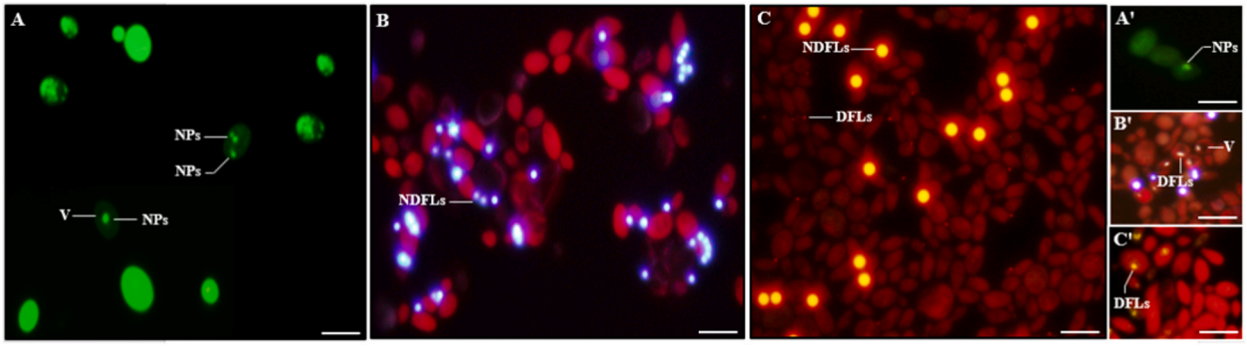

Fig. 5. Internalization of FITC- labelled nanoparticles (NPs) into *Candida albicans*. A and A′) Internalization of 70 nm gold NPs into the vacuole (V) of yeast cells. B and B′) Internalization of degraded 1000 nm Fluospheres (DFLs) into the yeast vacuole (V). C and C′) Internalization of degraded 2000 nm Fluospheres (DFLs) into the yeast vacuole (V). Non-degraded Fluospheres (NDFLs) remained intact and attached to the surface of yeast cells. Original magnification × 1000. Scale Bar: 5 μm. (For interpretation of the references to colour in this figure legend, the reader is referred to the Web version of this article.)

yeast cell, due to their large size, or degraded into smaller particles by the yeasts cocktail of secretory enzymes, internalized and ended up inside the vacuole of yeasts cells (% 90–100) (Fig. 6A1–B4). Uptake of degraded Fluospheres occurred 30 s after treatment and longer exposure led to increased accumulation of degraded Fluospheres. Fluorescence microscopy observations showed that Fluospheres with the size of 1000 and 2000 nm were similarly internalized into *C. albicans*, 30 s after treatment (% 90–100) (Fig. 5B, B′, C and C′). Interestingly, examination of Fluosphere-treated yeasts after 120 min showed that most of the yeast cells became brightly fluorescent due to internalization of more degraded 1000 or 2000 Fluospheres (Fig. 7A and B).

Uptake of degraded fluospheres by all the yeast cells showed no limitation in their internalization, compared with gold and albumin NPs. Internalization of inert carboxylated polysterene Fluospheres could be facilitated by their adhesion to polysaccharide networks of fungal cell wall as a nonspecific adhesive surface [46]. Furthermore, having –COOH functional groups may have increased the negative charge of Fluospheres, enhancing their internalization [47].

3.2.5. *Utilization of fluospheres as carbon source*

Compared with no growth on control medium, *C. tropicalis* showed confluent growth on Fluospheres solid medium by assimilation of carboxylated polysterene as a sole source of carbon (Fig. 8A and B). Fungi as the major decomposers of natural polymers such as cellulose and lignin [48,49] are able to degrade synthetic polymers such as polystyrene and metabolize it as a carbon source for growth [50]. AlkB family of hydroxylases [51] and hydroquinone peroxidase [52] have been shown to be involved in biodegradation of polystyrene.

4. Conclusion

Considering the estimated size of fungal cell wall pores as 200–400 nm, it appears that transport of small particles such as positively- charged 45 nm gold NPs occurs freely through the cell wall but larger 70 nm positively-charged or 100 nm negatively-charged NPs show limited internalization and positively-charged 100 nm NPs destroy the yeast cell. These results indicate that although the size of these particles is within the range of cell wall pore size, their physicochemical properties and interaction with the cell wall limit their internalization. In the other words, internalization of degraded Fluospheres indicates that although they are inert to negatively-charged, their other properties such as small size and chemical nature allow them to internalize. Here yeast's secretory enzymes play critical role in degrading them into smaller particles.

It is concluded that in fungi, lipid bilayer structure of EVs that can compress, as well as cell wall pores that can enlarge are involved in transport of large particles, including bacterial cell, across the cell wall. It seems that being encased in EVs serves as a pass word for facilitated export of different particles. It seems that membrane-encased exit protects the intracellular bacteria against stressful conditions such as exposure to antimicrobials or host immune system [53]. Release as free or vesicle-encased, could be regarded as an evolutionary innovation by intracellular bacteria for export without destruction of the host that is the fundamental principle of symbiotic relationship in which both yeast and bacterial partners survive. Accordingly, EVs-based approaches may be designed in order to develop new methods to treat fungal and bacterial diseases.

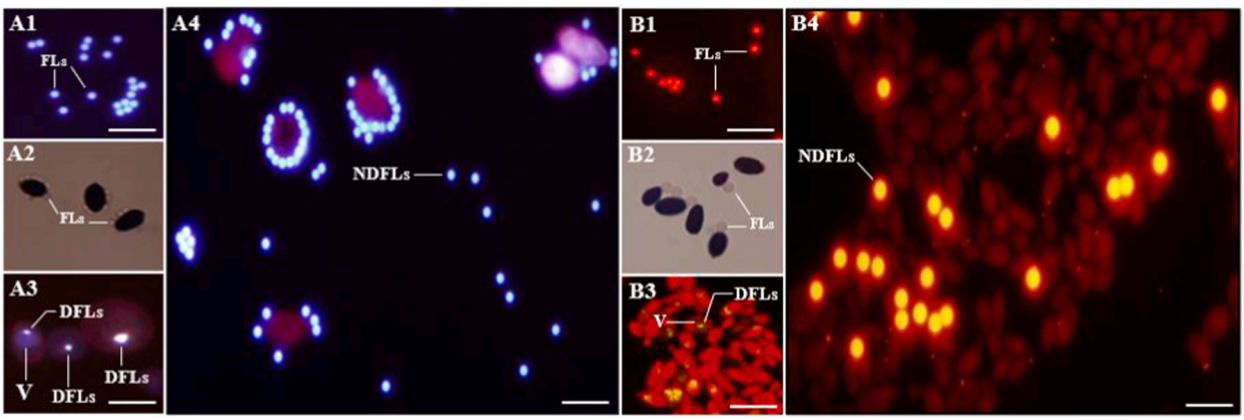

Fig. 6. Internalization of degraded 1000 and 2000 nm Fluospheres (DFLs) into *Candida tropicalis*. A1) The 1000 nm fluorescent Fluospheres (FLs). A2) Light microscopy of Gram- stained *C. tropicalis* treated with 1000 nm FLs showed their attachment to the surface of intact yeast cells. A3) Degraded 1000 nm FLs (DFLs) internalized into the vacuole (V) of yeast cell. A4) Non-degraded 1000 nm FLs (NDFLs) remained attached to the surface of yeast cell. B1) The 2000 nm fluorescent Fluospheres (FLs). B2) Light microscopy of Gram- stained *C. tropicalis* treated with 2000 nm FLs showed their attachment to the surface of intact yeast cells. B3) Degraded 2000 nm FLs (DFLs) internalized into the vacuole (V) of yeast cell. B4) Non-degraded 2000 nm FLs (NDFLs) remained attached to the surface of yeast cell. Original magnification of A1, A3, A4, B1, B3 and B4: × 1000. Original magnification of A2 and B2: × 1250. Scale Bar: 5 μm.

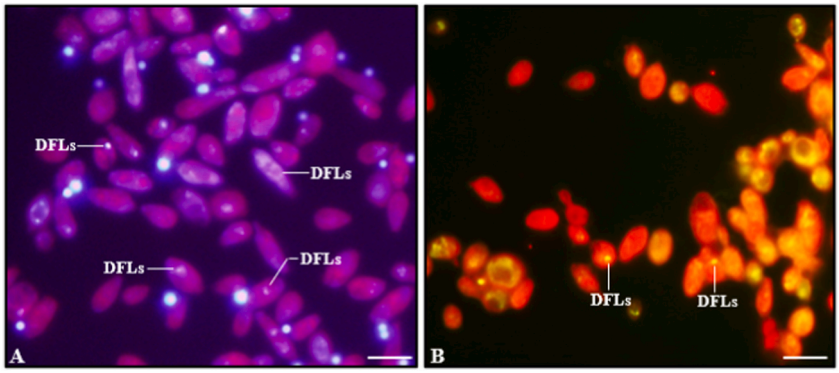

Fig. 7. Internalization of degraded 1000 and 2000 nm Fluospheres (DFLs) into *Candida tropicalis* after longer exposure time. Almost all the yeast cells became brightly fluorescent due to internalization of degraded 1000 nm (A) and 2000 nm (B) FLs (DFLs). Original magnification × 1000. Scale Bar: 5 μm.

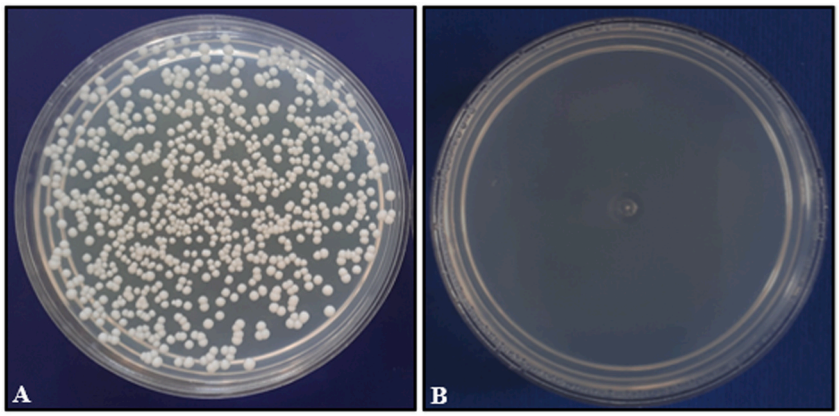

Fig. 8. Assimilation of Fluosphere as a carbon source. Growth of *Candida tropicalis* on the Fluosphere agar (A). No growth occurred on control medium without Fluosphere (B).

Author contribution statement

Farideh Siavoshi: Conceived and designed the experiments; analysed and interpreted the data; wrote the paper.

Hoda Ebrahimi: Conceived and designed the experiments; performed the experiments; analysed and interpreted the data; wrote the paper.

Mir Hadi Jazayeri: Contributed reagents, materials, analysis tools or data.

Abdolfattah Sarrafnejad: Contributed reagents, materials, analysis tools or data.

Parastoo Saniee: Contributed reagents, materials, analysis tools or data.

Maryam Mobini: Contributed reagents, materials, analysis tools or data.

Funding statement

This research did not receive any specific grant from funding agencies in the public, commercial, or not-for-profit sectors.

Data availability statement

Data included in article/supplementary material/referenced in article.

Declaration of interest's statement

The authors declare that they have no known competing financial interests or personal relationships that could have appeared to influence the work reported in this paper.

Additional information

No additional information is available for this paper.

References

[1] V. Ahmadjian, The Lichen Symbiosis, John Wiley & Sons, 1993.
[2] K. Sen, P. Sinha, S. Lahiri, Time dependent formation of gold nanoparticles in yeast cells: a comparative study, Biochem. Eng. J. 55 (1) (2011) 1–6, https://doi.org/10.1016/j.bej.2011.02.014.
[3] R.A. Hall, N.A. Gow, Mannosylation in C andida albicans: role in cell wall function and immune recognition, Mol. Microbiol. 90 (6) (2013) 1147–1161, https://doi.org/10.1111/mmi.12426.
[4] L. Walker, et al., The viscoelastic properties of the fungal cell wall allow traffic of AmBisome as intact liposome vesicles, mBio 9 (1) (2018), e02383-17, https://doi.org/10.1128/mbio.02383-17.
[5] A. Stirke, et al., The link between yeast cell wall porosity and plasma membrane permeability after PEF treatment, Sci. Rep. 9 (1) (2019) 1–10, https://doi.org/10.1038/s41598-019-51184-y.
[6] A. Casadevall, et al., Vesicular transport across the fungal cell wall, Trends Microbiol. 17 (4) (2009) 158–162, https://doi.org/10.1016/j.tim.2008.12.005.
[7] J. Liu, Q. Ru, Y. Ding, Glycation a promising method for food protein modification: physicochemical properties and structure, a review, Food Res. Int. 49 (1) (2012) 170–183, https://doi.org/10.1016/j.foodres.2012.07.034.
[8] N.A. Gow, J.-P. Latge, C.A. Munro, The Fungal Cell Wall: Structure, Biosynthesis, and Function, The fungal Kingdom, 2017, pp. 267–292, https://doi.org/10.1128/microbiolspec.funk-0035-2016.
[9] L.P. Erwig, N.A. Gow, Interactions of fungal pathogens with phagocytes, Nat. Rev. Microbiol. 14 (3) (2016) 163–176, https://doi.org/10.1038/nrmicro.2015.21.
[10] N. Pandey, M.K. Gupta, R. Tilak, Extracellular hydrolytic enzyme activities of the different Candida spp. isolated from the blood of the Intensive Care Unit-admitted patients, J. Lab. Phys. 10 (4) (2018) 392, https://doi.org/10.4103/JLP.JLP_81_18.
[11] M. Colombo, G. Raposo, C. Théry, Biogenesis, secretion, and intercellular interactions of exosomes and other extracellular vesicles, Annu. Rev. Cell Dev. Biol. 30 (2014) 255–289, https://doi.org/10.1146/annurev-cellbio-101512-122326.
[12] D.S. Choi, et al., Proteomics of extracellular vesicles: exosomes and ectosomes, Mass Spectrom. Rev. 34 (4) (2015) 474–490, https://doi.org/10.1002/mas.21420.
[13] A.M. Nicola, S. Frases, A. Casadevall, Lipophilic dye staining of Cryptococcus neoformans extracellular vesicles and capsule, Eukaryot. Cell 8 (9) (2009) 1373–1380, https://doi.org/10.1128/ec.00044-09.
[14] M.R. Bleackley, C.S. Dawson, M.A. Anderson, Fungal extracellular vesicles with a focus on proteomic analysis, Proteomics 19 (8) (2019), 1800232, https://doi.org/10.1002/pmic.201800232.
[15] J. Rizzo, M.L. Rodrigues, G. Janbon, Extracellular vesicles in fungi: past, present, and future perspectives, Front. Cell. Infect. Microbiol. 10 (2020) 346, https://doi.org/10.3389/fcimb.2020.00346.
[16] R. de Souza Pereira, J. Geibel, Direct observation of oxidative stress on the cell wall of Saccharomyces cerevisiae strains with atomic force microscopy, Mol. Cell. Biochem. 201 (1–2) (1999) 17–24, https://doi.org/10.1023/a:1007007704657.
[17] M.L. Rodrigues, et al., Vesicular polysaccharide export in Cryptococcus neoformans is a eukaryotic solution to the problem of fungal trans-cell wall transport, Eukaryot. Cell 6 (1) (2007) 48–59, https://doi.org/10.1128/ec.00318-06.
[18] D.L. Oliveira, et al., Extracellular vesicles from Cryptococcus neoformans modulate macrophage functions, Infect. Immun. 78 (4) (2010) 1601–1609, https://doi.org/10.1128/iai.01171-09.
[19] S. Heydari, et al., Helicobacter pylori Release from Yeast as a Vesicle-encased or Free Bacterium, Helicobacter, 2020, e12725, https://doi.org/10.1111/hel.12725.
[20] P. Saniee, et al., Immunodetection of Helicobacter pylori-specific proteins in oral and gastric Candida yeasts, Arch. Iran. Med. (AIM) 16 (11) (2013).
[21] F. Siavoshi, et al., Sequestration inside the yeast vacuole may enhance Helicobacter pylori survival against stressful condition, Infect. Genet. Evol. (2019), https://doi.org/10.1016/j.meegid.2019.01.029.
[22] F. Siavoshi, P. Saniee, Vacuoles of Candida yeast as a specialized niche for Helicobacter pylori, World J. Gastroenterol.: WJG 20 (18) (2014) 5263, https://doi.org/10.3748/wjg.v20.i18.5263.
[23] C.D. Smith, et al., Survival characteristics of diarrheagenic Escherichia coli pathotypes and Helicobacter pylori during passage through the free-living ciliate, Tetrahymena sp, FEMS Microbiol. Ecol. 82 (3) (2012) 574–583, https://doi.org/10.1111/j.1574-6941.2012.01428.x.
[24] R. Raghu Nadhanan, C.J. Thomas, Colpoda secrete viable L isteria monocytogenes within faecal pellets, Environ. Microbiol. 16 (2) (2014) 396–404, https://doi.org/10.1111/1462-2920.12230.
[25] M. Brandl, et al., Enhanced survival of Salmonella enterica in vesicles released by a soilborne Tetrahymena species, Appl. Environ. Microbiol. 71 (3) (2005) 1562–1569, https://doi.org/10.1128/aem.71.3.1562-1569.2005.
[26] J. Chen, et al., Legionella effectors that promote nonlytic release from protozoa, Science 303 (5662) (2004) 1358–1361, https://doi.org/10.1126/science.1094226.
[27] M. Hagedorn, et al., Infection by tubercular mycobacteria is spread by nonlytic ejection from their amoeba hosts, Science 323 (5922) (2009) 1729–1733, https://doi.org/10.1126/science.1169381.
[28] A. Flieger, et al., Pathways of host cell exit by intracellular pathogens, Microbial. Cell 5 (12) (2018) 525, https://doi.org/10.15698/mic2018.12.659.
[29] K. Ireton, H. Van Ngo, M. Bhalla, Interaction of microbial pathogens with host exocytic pathways, Cell Microbiol. 20 (8) (2018), e12861, https://doi.org/10.1111/cmi.12861.
[30] N. Moebius, et al., Active invasion of bacteria into living fungal cells, Elife 3 (2014), e03007, https://doi.org/10.7554/eLife.03007.
[31] P. Saniee, F. Siavoshi, Endocytotic uptake of FITC-labeled anti-H. pylori egg yolk immunoglobulin Y in Candida yeast for detection of intracellular H. pylori, Front. Microbiol. 6 (2015) 113, https://doi.org/10.3389/fmicb.2015.00113.
[32] C. Carvalho, et al., Yeast species associated with honey: different identification methods, Arch. Zootec. 59 (225) (2010) 103–113, https://doi.org/10.4321/S0004-05922010000100011.
[33] G. Frens, Controlled nucleation for the regulation of the particle size in monodisperse gold suspensions, Nat. Phys. Sci. 241 (105) (1973) 20–22. https://ui.adsabs.harvard.edu/link_gateway/1973NPhS..241...20F/doi:10.1038/physci241020a0.
[34] W. Haiss, et al., Determination of size and concentration of gold nanoparticles from UV− Vis spectra, Anal. Chem. 79 (11) (2007) 4215–4221, https://doi.org/10.1021/ac0702084.
[35] T. Aghaie, et al., Gold nanoparticles and polyethylene glycol alleviate clinical symptoms and alter cytokine secretion in a mouse model of experimental autoimmune encephalomyelitis, IUBMB Life 71 (9) (2019) 1313–1321, https://doi.org/10.1002/iub.2045.
[36] M.H. Jazayeri, et al., Colorimetric detection based on gold nano particles (GNPs): an easy, fast, inexpensive, low-cost and short time method in detection of analytes (protein, DNA, and ion), Sens. Bio-sens. Res. 20 (2018) 1–8, https://doi.org/10.1016/j.sbsr.2018.05.002.
[37] K. Zhang, et al., Fluorescent Imaging for Nano-Detection (FIND) of Cancer Cells, 2011.
[38] E.J. Lim, et al., Visualization of microscale particle focusing in diluted and whole blood using particle trajectory analysis, Lab Chip 12 (12) (2012) 2199–2210, https://doi.org/10.1039/C2LC21100A.
[39] S. Heydari, et al., Coniochaeta fungus benefits from its intracellular bacteria to form biofilm and defend against other fungi, Arch. Microbiol. 203 (4) (2021) 1357–1366, https://doi.org/10.1007/s00203-020-02122-4.

[40] H. Ebrahimi, et al., Yeast engineered translucent cell wall to provide its endosymbiont cyanobacteria with light, Arch. Microbiol. (2020) 1–9, https://doi.org/10.1007/s00203-020-01835-w.
[41] A. Tavakolian, F. Siavoshi, F. Eftekhar, Candida albicans release intracellular bacteria when treated with amphotericin B, Arch. Iran. Med. 21 (5) (2018) 191–198.
[42] R.P. Da Silva, et al., Extracellular vesicle-mediated export of fungal RNA, Sci. Rep. 5 (2015) 7763, https://doi.org/10.1038/srep07763.
[43] A. Jeyaram, S.M. Jay, Preservation and storage stability of extracellular vesicles for therapeutic applications, AAPS J. 20 (1) (2018) 1–7, https://doi.org/10.1208/s12248-017-0160-y.
[44] C. Ballou, Structure and Biosynthesis of the Mannan Component of the Yeast Cell Envelope, in: Advances in Microbial Physiology, Elsevier, 1976, pp. 93–158, https://doi.org/10.1016/s0065-2911(08)60227-1.
[45] L. Nimrichter, et al., Self-aggregation of Cryptococcus neoformans capsular glucuronoxylomannan is dependent on divalent cations, Eukaryot. Cell 6 (8) (2007) 1400–1410, https://doi.org/10.1128/ec.00122-07.
[46] S. Frases, et al., Capsule of Cryptococcus neoformans grows by enlargement of polysaccharide molecules, Proc. Natl. Acad. Sci. USA 106 (4) (2009) 1228–1233, https://doi.org/10.1073/pnas.0808995106.
[47] G.A. Holzapfel, Determination of material models for arterial walls from uniaxial extension tests and histological structure, J. Theor. Biol. 238 (2) (2006) 290–302, https://doi.org/10.1016/j.jtbi.2005.05.006.
[48] D.N. Georgiadou, et al., Microbial bioprospecting for lignocellulose degradation at a unique Greek environment, Heliyon 7 (6) (2021), e07122, https://doi.org/10.1016/j.heliyon.2021.e07122.
[49] G. Janusz, et al., Lignin degradation: microorganisms, enzymes involved, genomes analysis and evolution, FEMS Microbiol. Rev. 41 (6) (2017) 941–962, https://doi.org/10.1093/femsre/fux049.
[50] O. Motta, et al., Utilization of chemically oxidized polystyrene as co-substrate by filamentous fungi, Int. J. Hyg Environ. Health 212 (1) (2009) 61–66, https://doi.org/10.1016/j.ijheh.2007.09.014.
[51] H.J. Jeon, M.N. Kim, Functional analysis of alkane hydroxylase system derived from Pseudomonas aeruginosa E7 for low molecular weight polyethylene biodegradation, Int. Biodeterior. Biodegrad. 103 (2015) 141–146, https://doi.org/10.1016/j.ibiod.2015.04.024.
[52] Y. Zhang, et al., Biodegradation of polyethylene and polystyrene: from microbial deterioration to enzyme discovery, Biotechnol. Adv. (2022), 107991, https://doi.org/10.1016/j.biotechadv.2022.107991.
[53] K. Hybiske, R.S. Stephens, Exit strategies of intracellular pathogens, Nat. Rev. Microbiol. 6 (2) (2008) 99–110, https://doi.org/10.1038/nrmicro1821.